# Comparison of Elastic Configurations for Energy Efficient Legged Locomotion

Jasmin James, Patrick Ross, David Ball, *Member, IEEE*

***Abstract*— Energy efficient locomotion with the amazing agility of humans and other animals remains a challenge for legged robots. Many existing joint mechanisms for legged robots use a serial configuration which gives compliance, however this may be sub-optimal for energy efficiency. This paper investigates the energy efficiency of legged joints for stationary jumping for three configurations of the elastic and actuator elements: series, parallel and without an elastic element. The key result is that significant energy savings are possible with a parallel configuration over the series and non-elastic configurations for the range of typical animal and robot properties: mass, stance duty and toe jump height. While there are large regions where the series arrangement is more energy efficient, these are outside typical duty cycles and will be affected by significant impact losses. The results are obtained by optimizing a set of equations to find the minimum energy losses for stationary jumping. The scripts to generate the results are available as open source software.**

## I. Introduction

Humans and other animals traverse challenging terrain with amazing agility and high energy efficiency - something that remains a challenge for legged robots. In recent years the performance of legged robots has improved in particular due to advances in stable controllable locomotion. However, many legged robots remain tethered or carry high power generators, limiting their utility. This poor energy efficiency of electromechanical legs compared to their biological equivalents is despite the highly efficient conversion of electrical energy into mechanical energy in modern actuators.

Legged mechanisms consisting of actuators and springs are analogous to the function of muscle fibers (actuators), ligaments and tendons (springs). Actuators provide the input power either through torque or force; springs store energy by providing a cyclic conversion between kinetic and potential energy. Actuators and springs can be configured in series, parallel or a combination of both for compliance and to exploit energy savings.

The most common approach for leg mechanisms is either a non-elastic actuator (NEA) configuration or a series elastic actuator (SEA) configuration [2]. Typical robotic legs make use of rotary actuators through high ratio gearboxes, necessitating the use of series elastic elements to mitigate impact forces. However, there have been recent developments in fully back-drivable linear actuators with high power densities, approaching human muscles [3]. Such actuators make a parallel elastic actuator (PEA) configuration practically realizable, since no series spring is required to protect the actuator. Recent works have experimentally shown the potential of the PEA configuration [4-8].

This paper investigates the energy efficiency of legged joints for series, parallel and non-elastic configurations of the elastic and actuator elements for stationary jumping across a range of mass, stance duty and toe jump height. The key contribution is that the PEA has significant energy savings over the SEA and NEA configurations for typical legged animals and robots. There are large regions where the SEA is more energy efficient, however these are outside typical duty cycles for jumping and running. These regions correspond to short explosive motions, although impact losses will become significant at low duty cycles. This result is in direct contrast to the design of most joint mechanisms for legged robots that use a serial arrangement. Our results are for stationary hopping, however these results are applicable for energetic legged running motion which has been shown to be equivalent to hopping [9].

The results in this paper are obtained by optimizing a set of equations to find the minimum energy losses across three parameters: mass, stance duty and toe jump height. The three configurations are compared across the same set of parameters to give relative results for particular design constraints. In particular, this analysis extends our previous work [10] to include the modeling of the inertial mass of the series spring and rotor which we demonstrate to have a significant effect on the energy efficiency. (Note that the moving part in a linear actuator is also called a rotor.) This analysis also includes the NEA configuration in the comparison, and removes the assumption that the body follows a particular motion.

The following section reviews the relevant background material. Section 3 includes the derivation of the energy losses for the configurations. Sections 4 and 5 present the experimental method and results including a discussion and comparison with other work. Section 6 has the conclusion.

## II. Background

There are a large variety of approaches to increasing the energy efficiency of legged robots. With regards to the joint, Seok et al [11] proposes several design principles for reducing energy losses, such as high torque density motors, low impedance transmission, energy regeneration, and minimizing leg inertia. The design principles allowed them to produce a running quadruped with a similar energy performance characteristic to a real animal. There are a number of other high level approaches to improving the robot's performance such as higher energy density batteries,

The authors are with the School of Electrical Engineering and Computer Science at the Queensland University of Technology, QLD, Australia (e-mail: jasmin.james@connect.qut.edu.au)

lowering the robot's mass, improving restitution losses with better contact material.

There have been numerous studies demonstrating the benefits of including elastic elements for legged robots. This includes improvements to compliance and energy efficiency. Experiments have shown that parallel elastic elements can lower power consumption for a bounding quadruped [4], a walking biped [6, 8] and a hopping monoped [7]. These results demonstrate that the parallel configuration is beneficial, however they do not provide a framework for comparison to other configurations. Grimmer et al [12] compares several elastic configurations and shows that the parallel element decreases peak power requirements and the series element decreases total energy requirements. This analysis contained a number of simplifying assumptions. Yesilevskiy et al [13] also compares elastic configurations, concluding that where there are large reflected inertias through a gearbox, the series configuration is most appropriate, largely due to impact losses. This analysis precludes the existence of fully back-drivable linear actuators.

Energy efficiency is critically important in the usefulness of powered prosthetic limbs as it has a direct effect on the number of batteries that the user must carry and the time between recharging. Most current prosthetic leg limbs have short operating times in the order of several hours. Several prosthetic limbs have elastic elements. However, the selection of the elastic configuration was driven by the need for simplicity rather than energy efficiency [14].

There is also significant interest in the ability to change the effective stiffness of a joint. Part of this inspiration comes from a study that demonstrated that human runners will change their effective leg stiffness when transitioning between surfaces of differing hardness [15]. This has inspired a variety of mechanisms that allow for adjustment of the joint's effective stiffness for series [16-20] and parallel [10] configurations.

## III. Derivation of Energy Losses for the Elastic Configurations

The Spring-Loaded Inverted Pendulum (SLIP) model [21] is a widely used model of legged locomotion, approximating the leg as an ideal spring supporting a point mass body. Hence, SLIP is a specific form of sinusoidal motion given physical parameters. In this paper we don't enforce the exact SLIP solution; instead, formulating the problem using the more general sinusoidal solution. However, note that it is possible for the solution to be SLIP motion if this is the most energy efficient solution. We integrate energy losses over the stance phase as no energy should be expended during the flight phase. This reduces the analytical solution to only considering a single set of equations of motion with known boundary conditions.

This section compares the energy losses for the SEA, PEA and NEA configurations. The most energy efficient configuration is the one where the least energy is consumed for the same work. The equations for energy loss for the three configurations are derived as functions of mass, maximum toe height and stance duration. The SEA includes the second mass as a ratio of the body mass to the rotor and spring mass. For this analysis, stationary jumping is considered with a configuration of a linear spring, mass, damper and actuator and each configuration is shown in Figure 1.

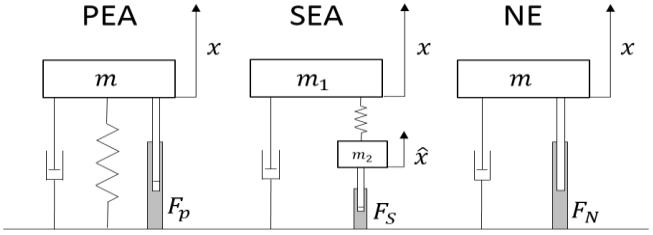


Figure 1. This figure shows the parallel elastic actuator (PEA), the series elastic actuator (SEA) and the non-elastic (NEA) configurations. The second mass in the SEA represents the spring and rotor. The SEA model is equivalent to one with the spring and actuator swapped. This form was chosen for simplicity in the analytical derivation.

In this work we focus on the losses due the actuator during stance, ignoring the impact losses. Raibert [22] concluded for a 2D planar hopper, of a similar form to this analysis, that the impact losses are proportional to the fraction of the total mass accounted for by the toe. In their application, impact losses were 5% of the total system energy corresponding to the fact that the toe was 5% of the total mass, whereas stance losses were much higher at 25% of the total system energy. This indicates that not only are impact losses much less significant than stance losses, but that they can also be mitigated by simply reducing the mass of the toe which is desirable for many other reasons.

### A. Force Models

This subsection derives the force models for the three configurations and provides practical limits for a realistic comparison.

Assuming $x$ follows a sinusoidal path the general form of $x$ for the body can be given by

$$x = -A\sin(\omega t + \sigma) + D \tag{1}$$

where $\omega$ is the frequency, $A$ is the amplitude, $\sigma$ is the phase offset and $D$ is the displacement. Assuming that the displacement at the beginning of the stance phase is equal to the displacement at the end gives the following equations

$$x(0) = x(T) \tag{2}$$

$$\dot{x}(0) = -\dot{x}(T) \tag{3}$$

where $T$ is the stance duration. This means that the work performed by the three configurations will be identical. Given these constraints the consistent solution is given by

$$\omega T + \sigma = 2\pi N + \pi - \sigma \tag{4}$$

where $N \in \mathbb{Z}$. If we consider only one period of motion, then $\omega$ can be constrained in terms of $\sigma$ and $T$ as

$$\omega = \frac{\pi - 2\sigma}{T} \tag{5}$$

Additionally by assuming a fixed jump height $h$ and solving for $\dot{x}(0)$ then $A$ can be constrained as

$$A = \frac{T\sqrt{2gh}}{(\pi - 2\sigma)\cos(\sigma)} \tag{6}$$

The force equations for the three configurations from Figure 1 are derived to be

$$F_P = m\ddot{x} + d\dot{x} + kx \tag{7}$$

$$F_S = m_2\ddot{\hat{x}} + k(\hat{x} - x) \quad (8)$$

$$F_N = m\ddot{x} + d\dot{x} \quad (9)$$

where $\hat{x}$ is given by

$$\hat{x} = x + \frac{m_1\ddot{x}}{k} + \frac{d\dot{x}}{k} \quad (10)$$

### B. Actuator losses

This subsection derives the actuator losses. In an electromechanical system the losses are predominantly due to the electrical resistance in the actuator. The power losses are given by

$$P = I^2R = \frac{F^2}{k_T^2}R \propto F^2 \quad (11)$$

where $I$ is the instantaneous current, $R$ is the coil resistance, $F$ is the instantaneous actuator force and $k_T$ is the torque constant of the linear actuator. This can be integrated over the stance phase to determine the energy losses.

$$E \propto \int_0^{\frac{2\pi}{w}} F^2 \quad (12)$$

For the PEA, by integrating Equation 7 and accounting for Equations 5 and 6 the actuator losses are given by

$$E_P \propto \frac{2\pi gh}{\cos^2(\sigma)}\left(\frac{m^2(\pi-2\sigma)}{T} + \frac{k^2T^3}{(\pi-2\sigma)^3} + \frac{(d^2-2mk)T}{(\pi-2\sigma)}\right) + \frac{2\pi k^2D^2T}{(\pi-2\sigma)} \quad (13)$$

Similarly for the SEA, by integrating Equation 8 while still accounting for Equations 5 and 6 gives

$$E_S \propto \frac{2\pi gh}{\cos^2(\sigma)}\left(\frac{m_1^2m_2^2}{k^2}\frac{(\pi-2\sigma)^5}{T^5} + \left(\frac{m_2^2d^2}{k^2} - \frac{2m_1m_2^2}{k} - \frac{2m_1^2m_2}{k}\right)\frac{(\pi-2\sigma)^3}{T^3} + \left(m_2^2 + m_1^2 + 2m_1m_2 - \frac{2m_2d^2}{k}\right)\frac{\pi-2\sigma}{T} + \frac{d^2T}{(\pi-2\sigma)}\right) \quad (14)$$

The NEA losses is given by integrating Equation 10 as

$$E_N \propto \frac{2\pi gh}{\cos^2(\sigma)}\left(\frac{m^2(\pi-2\sigma)}{T} + \frac{d^2T}{(\pi-2\sigma)}\right) \quad (15)$$

### C. Optimising the Losses

For the PEA the optimal value for $D$ in (1) was found by partially differentiating $E_P$ with respect to $D$ and solving for $\frac{\partial E}{\partial D} = 0$. This gives a minimum energy value for $D = 0$ and removes the last term from the energy equation for the PEA.

The equations for the optimal $k$ were derived the same way by partially differentiating with respect to the variables $k$ and $\sigma$ and solving for the PEA and SEA spring stiffnesses. The equation for optimal spring stiffness for the PEA gives

$$k_P = \frac{m\pi^2}{T^2} \quad (16)$$

and the SEA is given by

$$k_S = \frac{m_2\pi^2(T^2d^2 + \pi^2m1^2)}{T^2(T^2d^2 + \pi^2m_1^2 + \pi^2m_2m_1)} \quad (17)$$

These optimal spring stiffnesses are in many cases not physically realizable. In order for this model to be realised, constraints are applied to several parameters. This includes practical limits on the spring stiffness $k$, the deflection of the body $x$, and the deflection of the series spring $\hat{x}$ (which is the same as the deflection of the rotor mass $m_2$).

The spring constant $k$ is limited to a minimum of 1kNm$^{-1}$ which is a minimum realistic spring value. This limit prevents the optimal spring values from becoming unreasonably low at longer stance durations, often in the range of $10^{-2}$ Nm$^{-1}$.

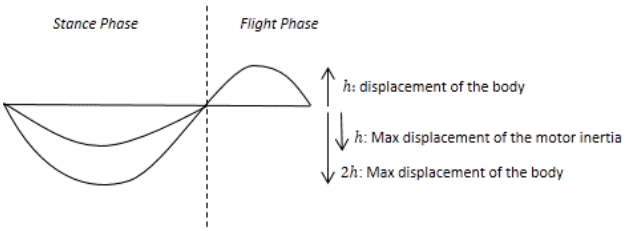


Figure 2. This diagram shows the constraints on the maximum displacement of the series spring and rotor and the maximum displacement of the body relative to jump height.

Providing a practical limit to the deflection of the body prevented unreasonable deflections of the body relative to the jump height. Following [23], an assumption was made that a reasonable maximum deflection for the three configurations is twice the jump height. This is a limit on the amplitude, $A$, of the body mass. Since $A$ is not a system parameter, Equation 6 has been rearranged to realise this limit in terms of $T$ and is given by

$$T < \frac{2h(\pi-2\sigma)\cos(\sigma)}{\sqrt{2gh}} \quad (18)$$

We specify an additional limit for the SEA on the deflection of the inertia mass, $D_{max}$ to prevent unreasonable deflections of the spring and rotor mass. This was assumed to be the jump height; which intuitively is less than the deflection of the body as shown in Figure 2. The limit on the amplitude of Equation 11 is given in terms of a minimum spring constant

$$k > \frac{D_{max}^2 + m_1^2\omega^2}{m_1 + \frac{1}{A\omega}\sqrt{-A^2d^2 + D_{max}^2d^2 + D_{max}^2m_1^2w^2}} \quad (19)$$

## IV. Experimental Method

In order to compare the energy losses for the series, parallel and non-elastic configurations the optimal spring constant $k$ was calculated. This value was then compared to the limits of the spring constant and the maximum inertia for the SEA in order keep the equations realizable, and set accordingly. The minimum energy values for $\sigma$ were found numerically using a constant set of parameters and a Nelder-Mead simplex direct search in MATLAB as a closed form solution was unable to be obtained. These optimal values were used in the three energy loss equations to give a function of the minimum $k$, the minimum $\sigma$ and the system parameters; mass, stance duty, and jump height.

Instead of varying the individual masses, the sum of the masses is fixed at $m_1 + m_2 = m$, and the variable $\alpha$ is introduced such that

$$\alpha = \frac{m_2}{m_1+m_2} \quad (20)$$

Stance duty is the ratio of the stance duration to the total cycle time. The results show the minimum energy solution and the most efficient configuration for a sweep of the mass, toe jump height and stance duration parameters. This is repeated for three values of $\alpha \in [0.1, 0.3, 0.6]$. The damping is fixed at 0.1 Nsm$^{-1}$ and the minimum spring constant is fixed at 1kNm$^{-1}$.

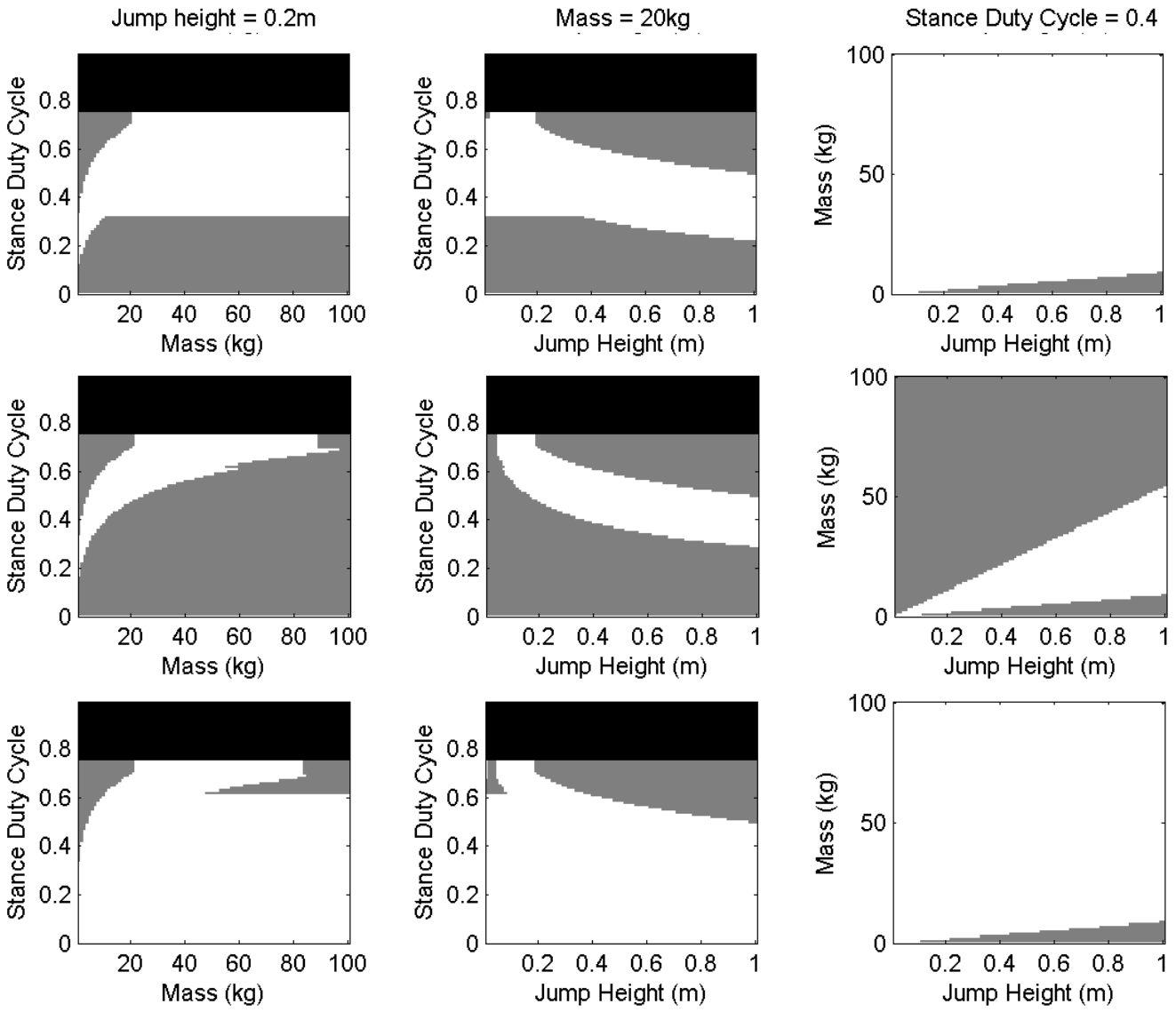


Figure 3. The figure shows three sets of graphs for the most efficient configuration for the parameter sweep. The efficient configuration show the regions where PEA (white) and the SEA (grey) are most efficient. The black represents the region with infeasible stance durations due to the maximum deflection criterion. The three sets of graphs represent (top to bottom) $\alpha = 0.1$, $\alpha = 0.3$ and $\alpha = 0.6$. The non-elastic configuration doesn't appear as it is never more efficient. Commonly the stance duty cycle (for both animals and robots) falls into the range of 0.35 - 0.45 [1], below which the unmodelled impact losses become significant.

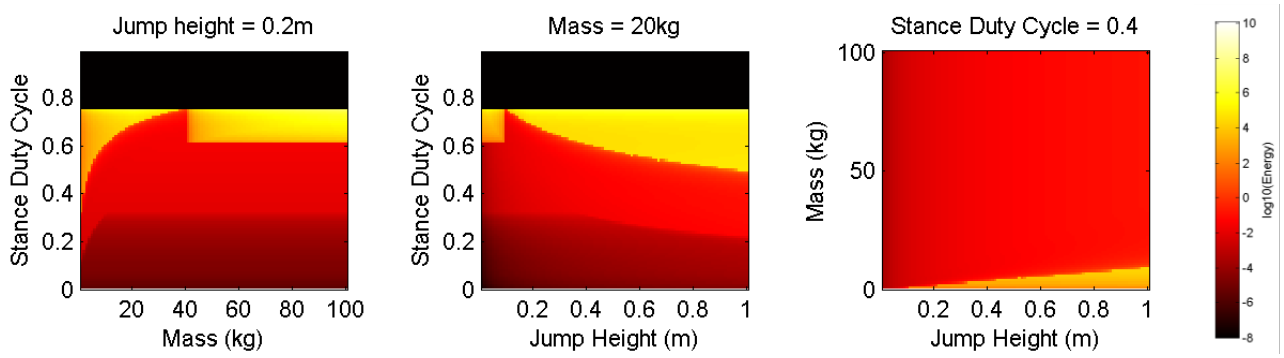


Figure 4. This shows the corresponding energy levels for the most efficient configurations where $\alpha = 0.1$ which is equivalent to animals and backdrivable actuators. There are significant jumps in the energy levels where due to the imposed limits the configurations are unable to reach their optimal spring stiffnesses. The lowest energy losses are for small stance duty. This figure can be compared to Figure 3 to see the optimal configuration.

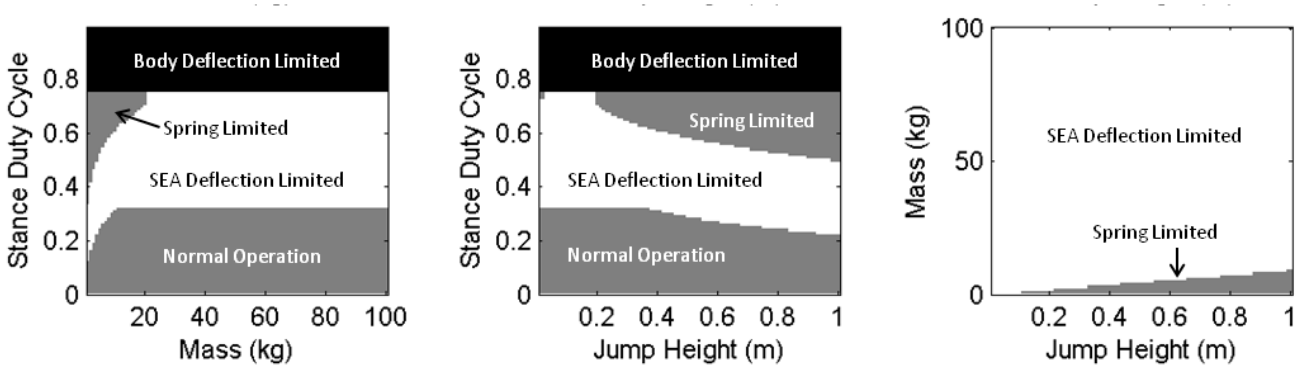


Figure 5. The different regions present in the $a = 0.1$ plots, showing the limits that are in effect in those regions. The significant limitation that allows the PEA to be more efficient is the limitation on the deflection of the SEA mass.

In order to explore the effects of considering the inertia of the motor for the SEA, the results include a sweep across $\alpha$ for fixed parameters.

The MATLAB scripts to generate the results are available online. (https://wiki.qut.edu.au/display/cyphy/Skippy,+the+robot+kangaroo)

## V. Results

Figure 3 shows the best configuration results for the sweep of mass, stance duty and toe jump height for the three configurations. The boundary between where the PEA and SEA are optimal has a complex shape in the stance duration. Above this limit the energy requirements for both SEA and PEA increase exponentially. This is the point where, due to the imposed limits, the optimization for the parallel arrangement is unable to reach the optimal spring stiffness $k$. The NEA does not appear on these plots as it is never more efficient than the other configurations.

Figure 4 shows the lowest energy losses are for small stance duty cycles. However, due to the assumption that the initial and final velocity of the body mass is equal in the stance phase, the model doesn't include impact losses, which become significant at short stance durations. These losses would have a substantial effect in lowering the energy efficiency in this lower band, and as such it would be ineffective to design energy efficient legged robots to operate within this region.

The lower regions show that the SEA is the most efficient for small stance ratios. This indicates that for short stance durations and explosive motions the SEA might be efficient if

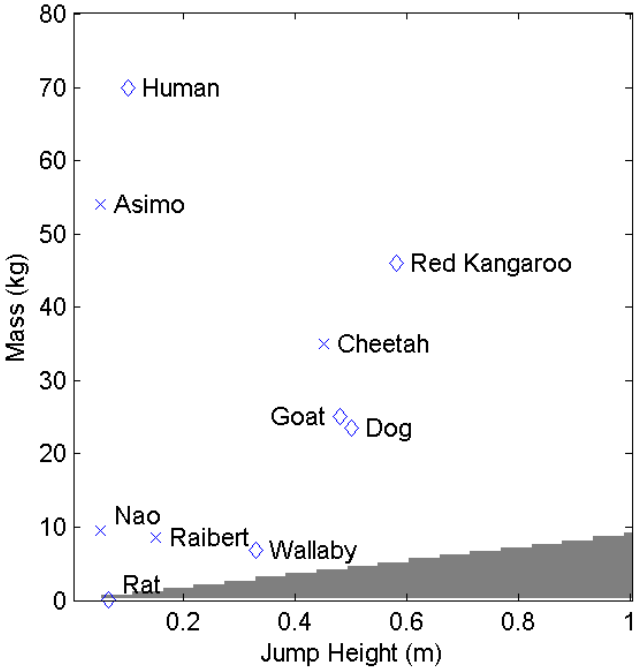


Figure 6. This graph shows where the PEA is more energy efficient (white) and where the SEA is more efficient (grey) for a range of mass and jump heights. Overlaid on this graph is the mass and jump height for animals (diamonds) and robots (crosses). The graphs shows that the region where the PEA is the most efficient is also the typical operating range for these animals and robots. Note the NEA does not appear in the figure as it is never more efficient. The details for the animals come from [1].

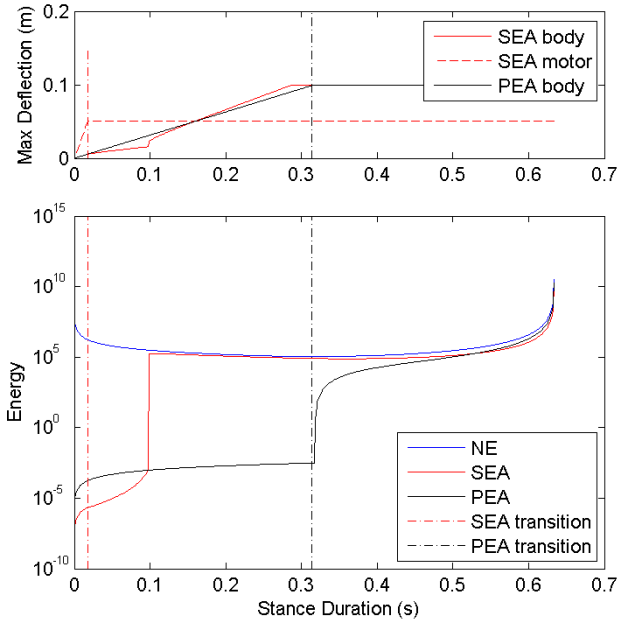


Figure 7. This graph shows the limiting effect of the maximum deflection and minimum spring constant on the energy losses. The dashed lines indicate the stance duration above which the maximum deflection criterion affects the result. The SEA transitions into sub-optimal spring constants significantly before the PEA, hence this region where the PEA is more efficient.

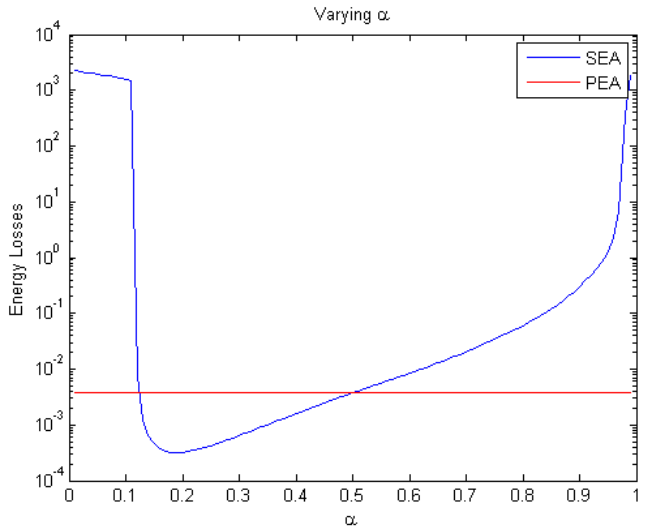


Figure 8. This graph compares the PEA with the SEA for a sweep of $\alpha$, which is the ratio of the body mass to the actuator inertial mass for the SEA. The result shows that the ratio in the SEA has a significant effect on the energy losses.

impact losses are small. The typical stance ratio for animals is in the range 0.35 – 0.45 [1]. This corresponds to the region where the PEA is the most efficient configuration.

For the sweeps of mass and jump height there is a linear relationship that defines the boundaries between the energy efficient SEA and PEA. The PEA is more energy efficient where $h < Cm$, where $C$ is a constant dependent on other system parameters. Figure 6 shows a number of animals and robots overlaid on a plot of the most efficient configuration. It can be seen that despite the presence of large regions where the SEA is more efficient, typical robots and animals are in a region where the PEA is the most efficient.

The effect of limiting the deflection of the inertia mass has the SEA transitioning into sub-optimal spring constants at much lower stance durations than the PEA. This effect is seen in Figure 7, indicated by the red dashed line. As the stance duration increases past this point the energy losses in the SEA increase rapidly, allowing the PEA to become more efficient. This effect continues up to the point where the body deflection limit causes both configurations to become sub-optimal (indicated by the black dashed line for the PEA).

### A. *Effect of SEA Actuator Inertia*

Figure 8 shows the effect of changing the ratio between the actuator and spring inertia and the body inertia for the SEA as compared to the PEA. It can be seen that when $\alpha$ is large or small the PEA is the most efficient choice, whereas there is a region of moderate values of $\alpha$ where the SEA becomes the most optimal choice.

Previous analyses have assumed that this mass is negligible ($\alpha = 0$), however, this figure shows that this is an important consideration for the SEA. Ignoring the inertia of the actuator can require as much as $10^6$ times more energy with all other things equal, compared to the minimum energy for an optimal choice of $\alpha$.

For many animals, an expected value for $\alpha$ would be very small. In electromechanical systems, small values of $\alpha$ correspond to fully back-drivable actuators without a gearbox, whereas large values of $\alpha$ correspond to actuators with a high reflected inertia through a high ratio gearbox. In both of these real world situations, the PEA is the more energy efficient choice. The region where the SEA is more efficient could be realized through a fully back-drivable actuator with additional inertia added to the rotor. However, the increased weight on the leg would likely lead to additional issues with balancing for a planar or unconstrained robot.

### B. *Comparison to other work*

Our conclusion that the PEA is more efficient is different from the result from Grimmer et al [12]. A fundamental difference is that their research focuses on prosthetic limbs for forward locomotion, whereas this work only considers whole body stationary jumping. In addition, there are two other differences that impact on the results. The first is that in this paper, the configurations are compared for energy losses using the same set of parameters for the three configurations. This allows a direct comparison, which gives a relative result for particular design constraints. The second is that the series model in this paper includes a second mass representing the rotor and spring. The previous subsection has shown that the ratio of this mass to the body mass makes a significant difference to energy losses.

## VI. Conclusion

The move towards highly efficiency legged robots will require research across a range of aspects such as increasing battery density, increasing actuator strength, design of optimal controllers, and minimizing mass and inertia. This paper presents an investigation of one aspect of designing joints for legged robots, namely the configuration of an elastic element and the actuator.

The results in the paper show where the PEA and SEA are the most efficient across key system parameters. However, all surveyed robots and animals fall into a region where the PEA is the most efficient for jumping motion. Intuitively, in the PEA, the spring will provide the majority of the force required by the joint, and the actuator need only supply the energy to account for the losses or deal with disturbances.

For very short stance durations the SEA is more efficient. This suggests that it is potentially more efficient for explosive motions, compared to the sustained motions for which the PEA is more efficient.

Our results show that the rotor and spring inertia has a substantial effect on the energy losses of the SEA. Consequently, high ratio gearboxes can have a remarkably detrimental effect on the overall energy efficiency of the SEA.

Future work will aim at extending this analysis to a running robot and validation with physical prototyping.

## References

[1] C. T. Farley, J. Glasheen, and T. A. McMahon, "Running springs: speed and animal size," *Journal of experimental Biology*, vol. 185, pp. 71-86, 1993.

[2] G. A. Pratt and M. M. Williamson, "Series elastic actuators," in *International Conference on Intelligent Robots and Systems*, 1995.

[3] B. P. Ruddy and I. W. Hunter, "A compact direct-drive linear synchronous motor with muscle-like performance," in *Robotics*

*and Automation (ICRA), 2013 IEEE International Conference on*, 2013, pp. 1498-1503.

[4] G. A. Folkertsma, S. Kim, and S. Stramigioli, "Parallel stiffness in a bounding quadruped with flexible spine," presented at the IEEE/RSJ International Conference on Intelligent Robots and Systems, Vilamoura, Algarve, Portugal, 2012.

[5] V. Duindam and S. Stramigioli, "Optimization of mass and stiffness distribution for efficient bipedal walking," in *Proceedings of IEEE/RSJ International Conference on Intelligent Robots and Systems, Edmonton, Canada*, 2005.

[6] T. Yang, E. R. Westervelt, J. P. Schmiedeler, *et al.*, "Design and control of a planar bipedal robot ERNIE with parallel knee compliance," *Autonomous Robots*, vol. 25, 2008.

[7] F. Gunther, Y. Shu, and F. Iida, "Parallel elastic actuation for efficient large payload locomotion," in *Robotics and Automation (ICRA), 2015 IEEE International Conference on*, 2015, pp. 823-828.

[8] A. Mazumdar, S. Spencer, J. Salton, *et al.*, "Using parallel stiffness to achieve improved locomotive efficiency with the Sandia STEPPR robot," in *Robotics and Automation (ICRA), 2015 IEEE International Conference on*, 2015, pp. 835-841.

[9] M. H. Raibert, J. Benjamin Brown, M. Chepponis, *et al.*, "Dynamically Stable Legged Motion," Massachusetts Institute of Technology, Cambridge1989.

[10] D. Ball, P. Ross, J. Wall, *et al.*, "A novel energy efficient controllable stiffness joint," in *Robotics and Automation (ICRA), 2013 IEEE International Conference on*, 2013, pp. 802-808.

[11] S. Seok, A. Wang, M. Y. Chuah, *et al.*, "Design principles for highly efficient quadrupeds and implementation on the MIT Cheetah robot," in *Robotics and Automation (ICRA), 2013 IEEE International Conference on*, 2013, pp. 3307-3312.

[12] M. Grimmer, M. Eslamy, S. Gliech, *et al.*, "A Comparison of Parallel- and Series Elastic Elements in an actuator for Mimicking Human Ankle Joint in Walking and Running," presented at the IEEE International Conference on Robotics and Automation, Minnesota, USA, 2012.

[13] Y. Yesilevskiy, W. Xi, and C. D. Remy, "A comparison of series and parallel elasticity in a monoped hopper," in *Robotics and Automation (ICRA), 2015 IEEE International Conference on*, 2015, pp. 1036-1041.

[14] J. K. Hitt, "An Active Foot-Ankle Prosthesis With Biomechanical Energy Regeneration," *Journal of medical devices*, vol. 4, 2010.

[15] D. P. Ferris, K. Liang, and C. T. Farley, "Runners adjust leg stiffness for their first step on a new running surface " *Journal of Biomechanics*, vol. 32, 1999.

[16] A. Jafari, N. G. Tsagarakis, and D. G. Caldwell, "AwAS-II: A new Actuator with Adjustable Stiffness based on the novel principle of adaptable pivot point and variable lever ratio," in *International Conference on Robotics and Automation (ICRA)*, Shanghai, China, 2011.

[17] A. Jafari, N. G. Tsagarakis, B. Vanderborght, *et al.*, "A Novel Actuator with Adjustable Stiffness (AwAS)," in *A Novel Actuator with Adjustable Stiffness (AwAS)*, Taipei, Taiwan, 2010.

[18] J. W. Hurst, J. E. Chestnutt, and A. A. Rizzi, "The Actuator With Mechanically Adjustable Series Compliance," *IEEE Transactions on Robotics*, vol. 26, 2010.

[19] B. Vanderborght, N. G. Tsagarakis, R. V. Ham, *et al.*, "MACCEPA 2.0: compliant actuator used for energy efficient hopping robot Chobino1D," *Autonomous Robots*, vol. 31, pp. 55-65, 2011.

[20] S. Wolf and G. Hirzinger, "A New Variable Stiffness Design: Matching Requirements of the Next Robot Generation," presented at the 2008 IEEE International Conference on Robotics and Automation, Pasadena, USA, 2008.

[21] T. A. McMahon and G. C. Cheng, "The mechanics of running: How does stiffness couple with speed? ," *Journal of Biomechanics*, vol. 23, 1990.

[22] M. H. Raibert, H. B. Brown, E. Hastings, *et al.*, "Dynamically Stable Legged Locomotion Second Report to DARPA," 1983.

[23] R. Blickhan, "The Spring-Mass Model for Running and Hopping," *Journal of Biomechanics*, vol. 22, pp. 1217-1227, 1989.